SECOND EUROPEAN CONFERENCE ON EARTHQUAKE ENGINEERING
AND SEISMOLOGY, ISTANBUL AUG. 25-29, 2014

WIND TURBINES IN SEISMIC ENVIRONMENT: A CASE STUDY

Jónas Thór SNÆBJÖRNSSON[1], Rajesh RUPAKHETY[2], and Ragnar SIGBJÖRNSSON[3]

ABSTRACT

The research objectives of the current study are to investigate and model the near-fault effects of earthquakes on wind turbines with horizontal axis of rotation. The presentation focuses on the experimental wind turbines recently installed in Iceland by the National Power Company of Iceland (Landsvirkjun). Each wind turbine has a 900 kW capacity and the generating capacity could be up to 2.7 GWh per year. The height of the mast is 55 m and the length of each blade measures 22 m. When the blades are at their highest position the total height is 77 m. The methodology outlined in the following is general and can be applied to any wind turbine (or wind farm) in an earthquake prone area where near-fault earthquake effects are of significance. The goal is to provide engineers with seismic design provissions for wind turbines in earthquake prone regions.

INTRODUCTION

Emphasis on renewable energy has been increasing worldwide over the past decade, including harnessing of wind energy using wind turbines. China is currently the largest country in terms of globally installed wind power, followed by U.S., India and Germany. On the other hand, the wind energy generation as a proportion of the electricity consumption is dominated by European countries with Denmark in the lead producing currently about 29% of its total energy consumption by wind turbines (Wiser and Bolinger, 2012). Many of these countries are seismically active regions which underlines the need to take earthquake action into consideration in the design process (Hanler et al., 2006; Prowell and Veers, 2009). There is currently a growing interest in harnessing the wind power in so-called wind farms—an infrastructure system consisting of relatively large, expensive, and homogeneous wind turbines—it is essential to minimise the probability of total shut-down. In this context, at a wind farm, an earthquake can potentially cause a collapse of every turbine within the farm. Consequently, some existing guidelines recommend designing the wind turbines as high safety class structures (EC8-1, 2004; Risø, 2002; DNV, 2013).

It should be pointed out that so far we have only considered the seismic effects on a single wind turbine. For a wind farm it is needed to take the spatial variability into consideration. The data needed in this case is obtained using small aperture array. Coherency derived from such data is displayed in Sigbjörnsson et al. (2013). Further analyses are on-going to minimise the risk of energy production disturbances due to earthquakes applying realistic layout of potential wind farms in the study area.

The research objective is to model and investigate the near-fault effects of earthquakes on wind turbines with horizontal axis of rotation. The aim is to provide engineers with seismic design guidelines for wind turbines in earthquake prone regions. The presentation focuses on the

[1] Professor, Reykjavik University, Menntavegur 1, Reykjavik, Iceland, jonasthor@ru.is
[2] Professor, Earthquake Engineering Research Center, 800 Selfoss, Iceland, rajesh@hi.is
[3] Professor, Earthquake Engineering Research Center, 800 Selfoss, Iceland, ragnar.sigbjornsson@hi.is

experimental wind turbines of Landsvirkjun located in the vicinity of the Burfell Hydroelectric Power Station. The methodology outlined is on the other hand general and can be applied to any earthquake prone area where near-fault earthquake effects are of significance.

SYSTEMS MODELLING

The equations of motion describing linear structural behaviour of wind turbines can, in principle, be represented within the framework of the finite element method as follows assuming viscous damping behaviour:

$$\mathbf{M}\ddot{\mathbf{r}} + \mathbf{C}\dot{\mathbf{r}} + \mathbf{K}\mathbf{r} = \mathbf{Q}(t) \tag{1}$$

Here, **M**, C and **K** are the system matrices describing the structural properties of the multi-component system, respectively mass, damping and stiffness; **r** is the structural response; and the vector **Q** represents the environmental action—including wind and earthquake excitation forces—and aeroelastic interaction given as a function of time *t*. In addition the **Q** vector includes soil-structure interaction, which is generally of importance especially for the seismic case. The above equation will also be applied in the current study to represent the linearised structural case.

Fluid structure interaction - Aeroelasticity

It is possible to express the excitation, $\mathbf{Q}(t)$, induced by a "mono-chromatic" harmonic excitation, taken to be proportional to $\exp(\mathrm{i}\omega t)$, by the following linear equation:

$$\mathbf{Q}(t) = \mathbf{M}^{(a)}(\omega)\ddot{\mathbf{r}} + \mathbf{C}^{(a)}(\omega)\dot{\mathbf{r}} + \mathbf{K}^{(a)}\mathbf{r} + \mathbf{Q}_{\boldsymbol{o}}^{(ex)}(\omega)\exp(\mathrm{i}\omega t) \tag{2}$$

Here, ω is the frequency of the harmonic behaviour, $\mathbf{M}^{(a)}$ is commonly denoted added mass (and is commonly omitted in aeroelastic analysis but must be included in the case of floating off-shore wind turbines), $\mathbf{C}^{(a)}$is sometimes referred to as aerodynamic damping; $\mathbf{K}^{(a)}$ is termed the aerodynamic stiffness; $\mathbf{Q}_{\boldsymbol{o}}^{(ex)}$ is termed the excitation amplitude. Within the framework of aeroelesticity the sum of the forces $\mathbf{M}^{(a)}(\omega)\ddot{\mathbf{r}} + \mathbf{C}^{(a)}(\omega)\dot{\mathbf{r}} + \mathbf{K}^{(a)}\mathbf{r}$ is commonly referred to as self-excited forces.

Substituting Eq.(2) into Eq.(1) and rearranging the terms gives:

$$\left[\mathbf{M} - \mathbf{M}^{(a)}(\omega)\right]\ddot{\mathbf{r}} + \left[\mathbf{C} - \mathbf{C}^{(a)}(\omega)\right]\dot{\mathbf{r}} + \left[\mathbf{K} - \mathbf{K}^{(a)}(\omega)\right]\mathbf{r} = \mathbf{Q}_{\boldsymbol{o}}^{(ex)}(\omega)\exp(\mathrm{i}\omega t) \tag{3}$$

Hence, the aeroelastic system can be modelled in terms of the classical dynamic equation, Eq.(1), by introducing $\left[\mathbf{M} - \mathbf{M}^{(a)}(\omega)\right]$ as the system mass matrix, $\left[\mathbf{C} - \mathbf{C}^{(a)}(\omega)\right]$ as the system damping matrix, and $\left[\mathbf{K} - \mathbf{K}^{(a)}(\omega)\right]$ as the system stiffness matrix. The complexity of this equation compared with Eq.(1) is apparently primarily related to the frequency dependence of the system matrices. However, within the framework of linear systems subjected to single harmonic excitation this does not pose any difficulties in the response analysis.

Frequency domain representation

A particular solution of Eq.(3) is most easily obtained in the frequency domain recognising that the model solution is a harmonic function given as $\mathbf{r} = \mathbf{X}_{\boldsymbol{o}}(\omega)\exp(\mathrm{i}\omega t)$, where $\mathbf{X}_{\boldsymbol{o}}$ is the response amplitude which in the general case must be a complex quantity to preserve the phase information of the response. Substituting this model solution into Eq.(3) the differential equation is reduced to the following algebraic equation:

$$\left[\left[\mathbf{K} - \mathbf{K}^{(h)}(\omega)\right] - \omega^2\left[\mathbf{M} - \mathbf{M}^{(h)}(\omega)\right] + \mathrm{i}\omega\left[\mathbf{C} - \mathbf{C}^{(h)}(\omega)\right]\right]\mathbf{X}_{\boldsymbol{o}}(\omega) = \mathbf{Q}_{\boldsymbol{o}}^{(h)}(\omega) \tag{4}$$

Here the aeroelastic properties of the combined system are furnished in:

$$\mathbf{D}(\omega) = \left[\left[\mathbf{K} - \mathbf{K}^{(h)}(\omega)\right] - \omega^2\left[\mathbf{M} - \mathbf{M}^{(h)}(\omega)\right] + \mathrm{i}\omega\left[\mathbf{C} - \mathbf{C}^{(h)}(\omega)\right]\right] \tag{5}$$

which sometimes is referred to as the "dynamic stiffness" of the system. The response induced by the "mono-chromatic" harmonic excitation is then obtained by inverting the dynamic stiffness matrix, i.e.:

$$\mathbf{X_o}(\omega) = \mathbf{H}(\omega)\mathbf{Q_o^{(h)}}(\omega) \tag{6a}$$

where, $\mathbf{H}(\omega)$ is the so-called frequency response function given as $\mathbf{H}(\omega) = \mathbf{D}^{-1}(\omega)$; and $\mathbf{X_o}(\omega)$ is the complex response amplitude.

The above presentation is only valid for the mono-chromatic harmonic excitation, which is not considered as a good approximation for real windy environment, which are random in nature. However, this type of modelling can be generalised, within the framework of linear systems, to incorporate excitation represented as a sum of finite number of harmonic components by virtue of the principle of superposition. The principle of superposition states: The response of a linear system at a given point in space and time induced by two or more stimuli is the sum of the responses induced by each stimulus individually. Hence, if input *A* induces response *X* and input *B* gives response *Y*, then input (*A* + *B*) results in response (*X* + *Y*). It follows that Eq.(4) applies also for environment represented by Fourier series. In the case of a stochastic wind field the excitation in the frequency domain can be obtained as the Fourier transform of the excitation time series. Therefore, Eq.(4) applies also in the case of random excitation.

In the general case the right hand side of Eq.(4) can be interpreted as the Fourier transform of the excitation forces, i.e. $\mathbf{Q}^{(h)}(\omega)$**,** where ω is treated as a continuous variable. Then, the solution can be expressed formally by Eq.(6a) as follows:

$$\begin{aligned}&\mathbf{X}(\omega) = \mathbf{H}(\omega)\mathbf{Q}^{(ex)}(\omega)\\ &\mathbf{H}(\omega) = \left[\left[\mathbf{K} - \mathbf{K}^{(a)}(\omega)\right] - \omega^2\left[\mathbf{M} - \mathbf{M}^{(a)}(\omega)\right] + \mathrm{i}\omega\left[\mathbf{C} - \mathbf{C}^{(a)}(\omega)\right]\right]^{-1}\end{aligned} \tag{6b}$$

Here, $\mathbf{Q}^{(ex)}$ is denoted the Fourier spectrum of the excitation, obtained by taking the Fourier transform of the excitation time series; $\mathbf{H}(\omega)$ is sometimes termed the "aeroelastic" frequency response function, while the "empty space" one is given as:

$$\mathbf{H}(\omega) = [\mathbf{K} - \omega^2\mathbf{M} + \mathrm{i}\omega\mathbf{C}]^{-1} \tag{6c}$$

The time series of the structural response are readily obtained taking the inverse Fourier transform of $\mathbf{X}(\omega)$**.** The statistics of any required response quantity can then be obtained by repeating the above described solution procedure for a comprehensive ensemble of excitation forces. An alternative to this type of procedure, which sometimes is referred to as Monte Carlo solution technique, exists in the well-known stochastic response analysis of linear systems proven to be very efficient if the excitation can be modelled as a stationary homogeneous Gaussian process.

Time domain representation

The above outlined modelling refers primarily to the frequency domain. However, it was indicated that the relation between the frequency domain and the time domain was furnished in the Fourier transform. Along these lines, it is possible to express a general time domain representation of the aeroelastic system by taking the inverse Fourier transform of Eq.(6b). That leads to the integro-differential equation given as follows, assuming causality:

$$\int_{-\infty}^{\infty}\mathbf{m}(t-\tau)\ddot{\mathbf{r}}(\tau)d\tau + \int_{-\infty}^{\infty}\mathbf{c}(t-\tau)\dot{\mathbf{r}}(\tau)d\tau + \int_{-\infty}^{\infty}\mathbf{k}(t-\tau)\mathbf{r}(\tau)d\tau = \mathbf{q}(t) \tag{7a}$$

Here, the $\mathbf{q}(t)$ is the excitation in the time domain; the following holds regarding the time dependent properties of the aeroelastic system matrices:

$$\mathbf{m}(t) = \frac{1}{2\pi}\int_{-\infty}^{\infty}\left(\mathbf{M} - \mathbf{M}^{(a)}(\omega)\right)e^{i\omega t}\,d\omega \tag{7b}$$

$$\mathbf{c}(t) = \frac{1}{2\pi}\int_{-\infty}^{\infty}\left(\mathbf{C} - \mathbf{C}^{(a)}(\omega)\right)e^{i\omega t}\,d\omega \tag{7c}$$

$$\mathbf{k}(t) = \frac{1}{2\pi}\int_{-\infty}^{\infty}\left(\mathbf{K} - \mathbf{K}^{(a)}(\omega)\right)e^{i\omega t}\,d\omega \tag{7d}$$

Furthermore, the particular time domain solution can be obtained as follows:

$$\mathbf{r}(t) = \int_{-\infty}^{\infty} \mathbf{h}(t-\tau)\mathbf{q}(\tau)d\tau \tag{2.8}$$

where, $\mathbf{h}(\cdot)$ is the so-called impulse response function of the aeroelastic system given as follows in terms of the frequency response function in Eq.(6b):

$$\mathbf{h}(t) = \frac{1}{2\pi}\int_{-\infty}^{\infty} \mathbf{H}(\omega)e^{i\omega t}\, d\omega \tag{2.9}$$

There exists several methods to solve Eq.(7) directly in the time domain. Such approaches are useful if it is needed to generalise the above formulation to cover inelastic behaviour or other nonlinear structural performance. A solution outlined by Øiseth et al. (2012) is based on the following expression neglecting the added mass which is generally without significance:

$$\mathbf{M}\ddot{\mathbf{r}}(t) + \int_{-\infty}^{\infty} \mathbf{c}(t-\tau)\dot{\mathbf{r}}(\tau)d\tau + \int_{-\infty}^{\infty} \mathbf{k}(t-\tau)\mathbf{r}(\tau)d\tau = \mathbf{q}(t) \tag{10}$$

This is a simplified procedure to include the motion dependent fluid-structure interaction in a traditional FE-beam formulation by augmentation of the number of degrees-of-freedom, which depends on the fluid-structure interaction derivatives for each case. This procedure has many advantages compared to other potential solution procedures suggested.

NATURAL MODES AND NATURAL FREQUENCIES

The natural frequencies and corresponding natural modes are of special interests. The damped natural frequencies and the corresponding natural modes can be obtained using the homogeneous counterpart of Eq.(1), i.e.:

$$\mathbf{M}\ddot{\mathbf{r}} + \mathbf{C}\dot{\mathbf{r}} + \mathbf{K}\mathbf{r} = \mathbf{0} \tag{11}$$

It is commonly assumed, within the field of civil engineering structural dynamics, that the structural damping is very small and that Eq.(11) can, hence, be reduce to:

$$\mathbf{M}\ddot{\mathbf{r}} + \mathbf{K}\mathbf{r} = \mathbf{0} \tag{12}$$

This leads to the classical eigenvalue problem, giving real undamped natural frequencies and real undamped natural mode shapes. The undamped natural modes are traditionally used as a generalised coordinates for classically damped system. Then it is possible to approximate the coupled equation of motion by a series of un-coupled second order equation each representing a single generalised degree of freedom.

To exemplify the natural modes and frequencies of the study we have developed a finite element models illustrated in Figure 1. The details of the finite element modelling are omitted herein. The results are given in Figure 2 displaying the first three natural modes of vibrations. The dynamic behaviour of the system is dominated by the fundamental mode, which is influenced significantly by the mass at the top (nacelle). The first two modes of vibration include over 90% of the effective mass.

If the fluid structure interaction is to be considered in the current case the result will be a non-classically damped system. Then the undamped natural frequencies of the aeroelastic system and the corresponding modes must be determined using the homogeneous counterpart of Eq.(3). That is:

$$\left[\mathbf{M} - \mathbf{M}^{(a)}(\omega)\right]\ddot{\mathbf{r}} + \left[\mathbf{C} - \mathbf{C}^{(a)}(\omega)\right]\dot{\mathbf{r}} + \left[\mathbf{K} - \mathbf{K}^{(a)}(\omega)\right]\mathbf{r} = \mathbf{0} \tag{13}$$

In this case the damping can't be neglected due to the aeroelasic contribution which is not necessarily small in the case of wind turbine. Therefore, it may not be possible to reduce this eigenvalue problem to the classical one mentioned above. The natural mode shape will in this case be complex quantities (see, for instance, Langen and Sigbjörnsson, 1979; Humar 2004).

(a) (b) (c) (d)

Figure 1. The study wind turbine: (a) the wind turbine in the natural surroundings; (b) view of the nacelle, (c) FE model without excentricity; (d) FE model with excentricity.

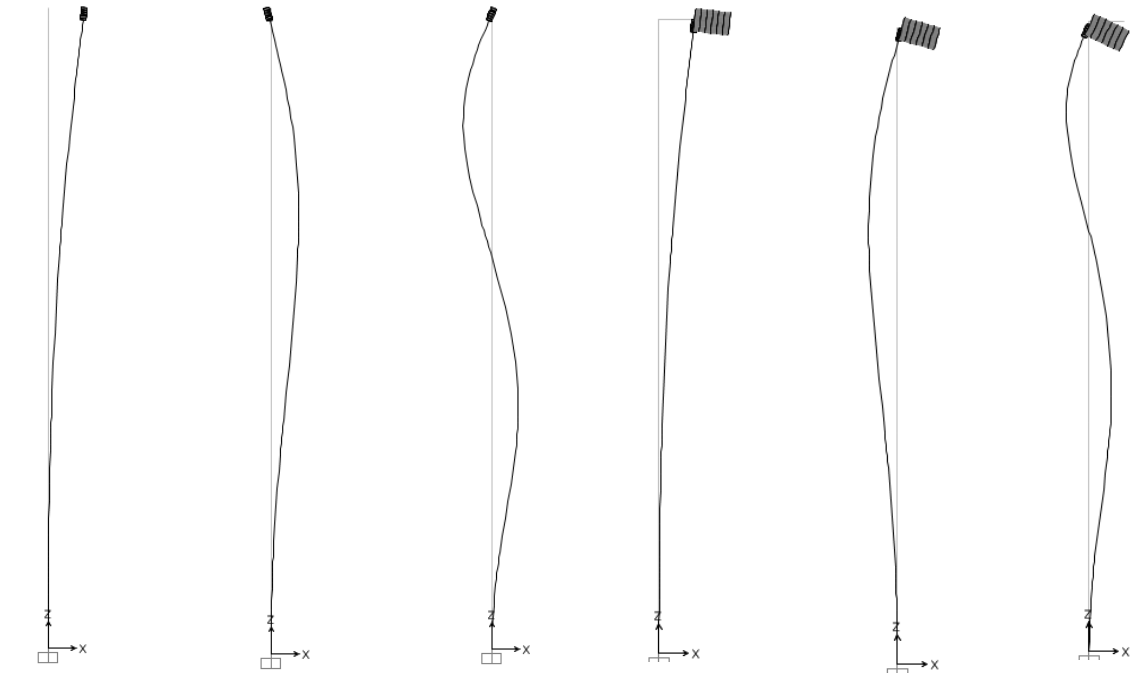

T_1 = 2.186 s T_2 = 0.275 s T_3 = 0.099 s T_1 = 2.191 s T_2 = 0.288 s T_3 = 0.113 s

(a) (b)

Figure 2. Undamped natural mode shapes and frequencies of the study wind turbine: (a) FE model without excentricity, (b) FE model with excentricity.

SEISMIC EXCITATION

The study site selected is *Hafið* where two experimental wind turbines have been erected, within the construction area of Búrfell Hydropower Station, in the south of Iceland. This area is prone to earthquakes originating in the eastern part of the South Iceland Seismic Zone. The magnitude of these earthquakes may reach magnitude 7; furthermore, the June 2000 South Iceland earthquakes were in the magnitude range 6.4-6.6 depending on reporting institutions. Characteristic for the South Iceland earthquakes are dominating near-fault pulses, which make the traditionally applied codified design procedures not applicable without modifications.

Near-fault ground motions are known to be a potential cause of severe damage to engineering structures. They usually carry a strong long-period pulse in their velocity records. Directivity effects and permanent displacement effects have been identified as the most common features of near-fault ground motions (Rupakhety et al. 2011). The most important model parameters characterising the directivity effects are related to the amplitude and frequency of the velocity pulse. The amplitude of the pulse is representative of the peak ground velocity. Different authors have defined the pulse period in different ways. Nevertheless, they have all found that the pulse period is linearly related to the seismic moment. It has also been found that the pulse period is closely related to the undamped period of single-degree-of-freedom (SDOF) system where the pseudo-velocity response spectrum (*PSV*) attains its maximum value. If the pulse were a simple harmonics with infinite duration, the peak of *PSV* would occur exactly at the pulse period. However, near-fault velocity pulses are of finite duration, defined by the pulse period and the number of half-cycles. Because of this, the period at which *PSV* is the maximum is a fraction of the pulse period, where the fraction depends on the number of half-cycles of the pulse. Apart from this, the presence of other components of ground motion not associated with the pulse itself can also cause the *PSV* to peak at a period different than the pulse period.

The first problem that arises in the quantification of directivity effects is the lack of Icelandic data. It has only been defined in roughly handful of records from 2000 and 2008. We therefore use an international database compiled by Rupakhety et al. (2011) containing strong-motion data from 29 different earthquakes, two of which are Icelandic. The magnitudes of these data are in the range 5.5 to 7.6 M_w. In total 93 records are analysed out of which seven come from the South Iceland Seismic Zone.

These data have been applied to establish relationship between the predominant period, T_d, and the seismic moment, M_w. The predominant period is defined as the period where 5% damped linear-elastic *PSV* reaches its peak value. If more than one peaks of comparable amplitude exist, then the longest period is considered. The period of the velocity pulse is related linearly to T_d. An advantage of using T_d is that, unlike pulse periods used in many simple pulse models, it can be unambiguously estimated. Since pulse period has been found to scale linearly with seismic moment, similar scaling for T_d is found. The relationship between T_d and M_w is herein modelled by:

$$\log(T_d) = 0.47\, M_w - 2.87 + n(0,0.18) \tag{14}$$

where the model parameters and the residual $n(0,0.18)$, denoting a Gaussian-distributed random variable with zero mean and standard deviation equal to 0.18, are obtained using least squares regression.

The second key quantity obtained from the database is peak-ground velocity (*PGV*). This quantity is related to the seismic moment and the distance to source through attenuation type model discussed by Rupakhety et al. (2011). The attenuation *PGV* is rather small for moderate sized earthquakes and short source distance, say, less than 5 km, which is in fair agreement with results reported by Bray and Rodriguez-Marek (2004) and Haldorsson et al. (2010).

The third key quantity is the earthquake response spectrum which is derived from the database. Regarding the lengthy and complex analysis the reader is referred to Rupakhety et al. (2011). The data is divided into six magnitude bins as summarised in Table 1 below.

Table 1. Grouping of near-fault records into six magnitude bins.

Bin	M_w range	No. of records
1	$5.5 < M_w \leq 6.0$	14
2	$6.0 < M_w \leq 6.3$	11
3	$6.3 < M_w \leq 6.6$	8
4	$6.6 < M_w \leq 6.8$	12
5	$6.8 < M_w \leq 7.3$	8
6	$7.3 < M_w \leq 7.6$	18

The normalised horizontal velocity response spectrum can be expressed as follows:

$$PSV_n(T_n, \zeta|M_w) = [I_1\{-0.5(\ln(T_n) + 1.4)^2\} + (4.92 - 0.58M_w)\{(1 - (T_n/T_d)^2)^2 + 4D_m^2(T_n/T_d)^2\}^{-0.5}]T_n \quad (15)$$

Here, T_n is undamped natural period, T_d is the predominant period, defined as the period where 5% damped linear-elastic *PSV* reaches its peak value, the parameters I_1 and D_m are given in Table 2 for the magnitude bins specified in Table 1.

Table 2. Parameters of the normalised velocity response spectrum, Eq.(15), for different magnitude bins (see Table 1) and critical damping ratio, ζ.

Bin	I_1	D_m
1	$0.320\zeta^{-0.5}$	$1.54\zeta + 0.39$
2	$0.239\zeta^{-0.5}$	$1.73\zeta + 0.44$
3	$0.211\zeta^{-0.5}$	$2.41\zeta + 0.47$
4	$0.204\zeta^{-0.5}$	$2.82\zeta + 0.50$
5	$0.283\zeta^{-0.5}$	$4.18\zeta + 0.58$
6	$0.242\zeta^{-0.5}$	$3.38\zeta + 0.59$

The pseudo-velocity response spectrum is hence obtained as:

$$PSV(T_n, \zeta|M_w) = PGV \cdot PSV_n(T_n, \zeta|M_w) \quad (16)$$

where *PGV* is the peak ground velocity, i.e. the normalisation coefficient. Hence, the pseudo-acceleration response spectrum is obtained using the spectral relation:

$$PSA(T_n, \zeta|M_w) = 2\pi\, PSV(T_n, \zeta|M_w)/T_n \quad (17)$$

In classical response spectrum analysis the acceleration response spectrum is assumed to be governing the excitation and the velocity response spectrum is disregarded. This is not necessarily the case for wind turbines and it is recommended that each case should be considered carefully.

The above outlined near-fault model is exemplified in Figure 2 where it is compared to Eurocode 8 type 1 standard spectrum. There is a significant difference between these two models. Eurocode 8 tends to overestimate the acceleration response for structures with undamped natural periods shorter than 0.5 s or there about. The overestimation can be up to 25% in the current case. On the other hand, Erocode 8 tends to underestimate the acceleration response for structures with periods

longer than 0.5 s. For the wind turbine discussed in Section 3 the current near-fault model leads to acceleration that approaches nearly twice the acceleration given by Eurocode 8. Based on further study along these lines, considering higher towers and bigger earthquakes, we conclude that the near-fault effects need to be taken into consideration in the design of wind turbines.

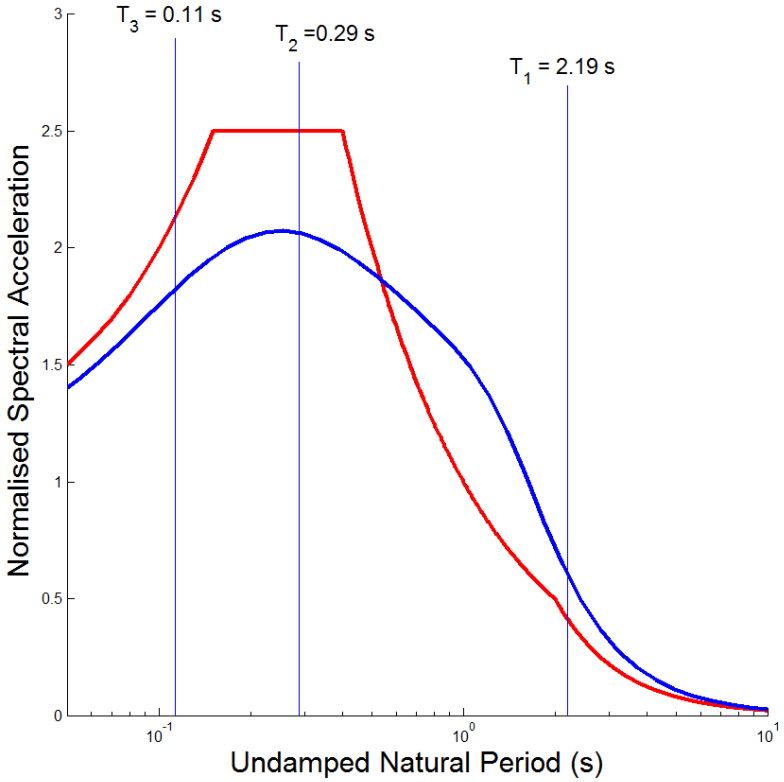

Figure 3. Normalised acceleration response spectrum induced by 6.5 magnitude earthquake: The blue curve is obtained using the above presented near-fault model; the red curve is Eurocode 8 type 1 model, which is independent of magnitude. The critical damping ratio is equal to 5%. The vertical brue lines represents three undamped natural periods of the wind turbine.

It should be pointed out that so far we have only considered the seismic effects on a single wind turbine. For a wind farm it is needed to take the spatial variability into consideration. This problem has been dealt with by Sigbjörnsson et al. (2013). However, further analyses are needed to minimise the risk of energy production disturbances for a realistic layout of potential wind farms.

MODELLING OF DAMPING

The structural system matrices **M** and **K** are easily determined within the finite element framework. The difficulties arise in the definition of the damping matrix **C.** The traditional approach in structural dynamics is to model the damping as a linear combination of the mass and the stiffness matrix. In this context it is worth mentioning the Rayleigh damping model, which is widely used in available standard software. More flexible models are furnished in the Wilson-Penzien approach (Wilson and Penzien, 1973) and application of Caughey series (Langen and Sigbjörnsson, 1979). These models make it possible to decouple the equation of motion by using the undamped natural modes. Such systems are termed classically damped systems. Then the critical damping ratio is apparently assumed to be given as follows (see, for instance, Damgaard et al., 2012):

$$\zeta = \zeta_{aero} + \zeta_{soil} + \zeta_{steel} \tag{18}$$

This is clearly an oversimplified model as it is assumed that the damping contributions are uniformly distributed throughout the entire system. This contradicts the observation that the wind turbine should be modelled as a multi-component system and the damping properties connected to the individual components. Hence, the aerodynamic damping model should be related to three components, i.e. (i) the blades, (ii) the tower, and the nacelle (or the housing containing the generating components in the wind turbine). The damping induced by the structural materials is related to three main components, i.e. the soil supporting the wind turbine, the steel material of the tower, and the material of the blades, usually polyester. This type of multi-component modelling leads to non-classically damped aeroelastic system. Hence, the classical techniques usually applied in structural dynamics do not apply. It is therefore recommended to base the response analysis on (i) the direct frequency response method using the full system matrices or (ii) the normal mode method applying the complex mode shapes (Langen and Sigbjörnsson, 1979). However, independent of the solution technique applied the information required to construct a realistic damping model is largely missing or incomplete, and was not found in the available literature. In the view of the authors such information can only be obtained by full scale field experiments

DISCUSSION AND CONCLUSIONS

It is clear that the wind field and the seismic waves can only be represented within the framework of stochastic processes. It is tradition within structural engineering and codified design to describe gusty wind as a Gaussian stochastic process. In that case the dynamic part of the process is described completely by the second order statistic of the field which is most commonly given in terms of the cross-spectral density. For a locally stationary and homogeneous seismic wave field a representation in the terms of the one-dimensional power spectral density and the coherency function and phase spectrum is commonly used. Along these lines the cross-spectral density of the seismic excitation forces, **q,** can be obtained in terms of the cross-spectral density (see Section 3). Then the cross-spectral density of the response is readily obtained by the following well known expression:

$$\mathbf{S_r}(\omega) = \mathbf{H}(\omega)\mathbf{S_q}(\omega)\mathbf{H}^*(\omega) \tag{19}$$

Here, the asterisk denotes complex conjugate and matrix transpose; $\mathbf{S_q}(\omega)$ is the cross-spectral density of seismic excitation; and $\mathbf{H}(\omega)$ is the (aeroelastic) frequency response function discussed above (see Section 2 and 3). This procedure is extremely simple when the fluid-structure interaction results in frequency dependent coefficients.

This procedure is strictly speaking only valid for linear or linearised systems. For the wind turbine dealt with in the appendices various nonlinearities may arise. The purpose of the proposed monitoring system is to define the applicability of the above described linear model and quantify potential nonlinearities. The effects of weak nonlinearities may appear as uncertainties in terms of residuals when fitting a linear system to recorded response data. A reduction of these uncertainties can be achieved by introducing stochastic averaging. It is worth mentioning two methods: Firstly, the stochastic linearization techniques, resulting in an equation set equivalent to Eq.(19). Secondly, the perturbation method yielding some additional terms to Eq.(19). Both these methods are computationally efficient. Furthermore, if the nonlinearities are not small higher order statistics may be required to achieve adequate results. In such cases Monte Carlo simulation techniques are also commonly considered, which in most cases, however, are more computationally demanding. In practical terms the earthquake induced response in the serviceability state is suggest described by the above stochastic representation using cross-spectral density to describe the second order statistics. In that case the effects of the frequency dependent parameters are judge to be significant. On the other hand it is assumed that nonlinear approach is required for the ultimate limit state conditions. Then Monte Carlo technique is the most tested procedure at hand, which is based on step-by-step solution procedures to generate the response time series. In that case it is required to perform appropriate response statistics on the generated time series.

AKNOWELEDGEMENTS

Partial financial support for this study was provided by the Landsvirkjun Energy Research Fund. Any opinions, findings and conclusions expressed in this paper are those of the authors and do not necessarily reflect the views of the funding agency.

REFERENCES

Damgaard, M., Ibsen, L.B., Andersen, L.V., and Andersen J.K.F. Cross-Wind Modal Properties of Offshore Wind Turbines Identified by Full Scale Testing. *Journal of Wind Engineering and Industrial Aerodynamics*, 116:94-108, 2013.

94–108, 2013.DNV. *Design of Offshore Wind Turbine Structures*. Det Norske Veritas AS, January 2013.

EC8-1. *Eurocode 8: Design of Structures for Earthquake Resistance – Part 1: General Rules Seismic Actions and Rules for Buildings*. European Committee for Standardisation, 2004.

Hanler, M., U. Ritschel, and I. Warnke. Systematic Modelling of Wind Turbine Dynamics and Earthquake Loads on Wind Turbines. *European Wind Energy Conference and Exhibition*, European Wind Energy Association, Athens, Greece, 2006.

Humar, J. L. *Dynamics of Structures.* CRC Press, 2005

Langen, I. and Sigbjörnsson, R. *Dynamisk analyse av konstruksjoner*, Tapir 1979.

Prowell, I., and P. Veers. *Assessment of Wind Turbine Seismic Risk: Existing Literature and Simple Study of Tower Moment Demand*. Technical report, Sandia National Laboratories, March 2009.

Prowell, I., M. Veletzos, A. Elgamal, and J. Restrepo. Experimental and Numerical Seismic Response of a 65-kW Wind Turbine. *Journal of Earthquake Engineering*, 13(8):1172–1190, 2009.

Risø. *Guidelines for Design of Wind Turbines*. Det Norske Veritas & Wind Energy Department of Risø National Laboratory, 2002.

Rupakhety, R., R Sigbjörnsson (2012). Spatial variability of strong ground motion:novel system-based technique applying parametric time series modelling, Bulletin of Earthquake Engineering 10:1193–1204, DOI 10.1007/s10518-012-9352-0

Rupakhety, R., R Sigbjörnsson (2013a). A note on autoregressive spectral estimates for frequency-wavenumber analysis of strong-motion array data, Bulletin of Earthquake Engineering, 11:1279-1285

Rupakhety, R., R. Sigbjörnsson (2013b) Rotation-invariant mean duration of strong ground motion. Bulletin of Earthquake Engineering, DOI 10.1007/s10518-013-9521-9

Sigbjörnsson, R., R Rupakhety, B Halldorsson, J T Snæbjornsson, S Olafsson (2013) The May 2008 Ölfus Earthquake in South Iceland: Modelling incoherence of strong ground motion. In Proceedings of the SE-50EE, International Conference on Earthquake Engineering, Skopje, Macedonia

Wiser, R. and M. Bolinger. *2011 Wind Technologies Market Report*. Technical Report No. TP-5000-53474 & DOE/GO-102009-2868, National Renewable Energy Laboratory, 2012.

Øiseth, O A, Rönnquist A, Sigbjörnsson R. Finite element formulation of the self-excited forces for time-domain assessment of wind-induced dynamic response and flutter stability limit of cable-supported bridges. *Finite Elements in Analysis and Design*, Vol. **50**, 2012, pp. 173–183